Persistent local chemical bonds in intermetallic phase formation

Yanwen Bai [a], Xiufang Bian [a,*], Xubo Qin [a], Shuo Zhang [b], Yuying Huang [b]

[a] *Key Laboratory for Liquid–Solid Structural Evolution and Processing of Materials, Ministry of Education, Shandong University, Jinan 250061, China*
[b] *Shanghai Synchrotron Radiation Facilities, Shanghai Institute of Applied Physics, Chinese Academy of Sciences, Shanghai 201204, China*

A B S T R A C T

We found a direct evidence for the existence of the local chemical Bi–In bonds in the $BiIn_2$ melt. These bonds are strong and prevail, dominating the structure evolution of the intermetallic clusters. From the local structure of the melt-quenched $BiIn_2$ ribbon, the chemical Bi–In bonds strengthen compared with those in the equilibrium solidified alloy. The chemical bonds in $BiIn_2$ melt retain to solid during a rapid quenching process. The results suggest that the intermetallic clusters in the melt evolve into the as-quenched intermetallic phase, and the intermetallic phase originates from the chemical bonds between unlike atoms in the melt. The chemical bonds preserve the chemical ordered clusters and dominate the clusters evolution.

© 2014 Elsevier B.V. All rights reserved.

1. Introduction

Known as important structural materials [1,2], the excellent physical properties, such as the superconductivity [3–5], the magnetic susceptibility [6,7], and the electrical resistivity [7], make the intermetallic compounds attract considerable attention. Recently, Wu and Li [8] reported the "intermetallic glasses" in the Cu–Zr system with near-intermetallic compositions. Then Wang et al. [9] explained the origin of these glass formers from the thermodynamics and kinetics points of view, using the melt fragility. Their research has explored new potential applications of the intermetallic alloys.

There is no doubt that the formation of the intermetallic alloys is critical to their performance. In these studies, concerned with the intermetallic compounds, one of the core issues is how to synthesize them with enhanced performance. Among the various synthetic methods [10–15], the intermetallic compounds are mostly formed in the liquid-phase reaction. Therefore, the behavior of the intermetallic compounds in the melt is crucial to the formation and performance of the materials. For example, Singh [16] and Prasad [17] have demonstrated that the Al_3Mg_2 intermetallic clusters in the liquid phase lead to the asymmetry in the properties of mixing of Al–Mg molten alloys. The large diversity of the physical properties of the solid Fe–Si system with different compositions is correlated with the changing volume fraction of the intermetallic clusters in the liquid [18]. When describing the liquid

structure in the whole concentration range in the Fe–Si [18] and Fe–Al [19] systems, the phase equilibrium diagrams of which are very complex, the intermetallic clusters have also been used as the important structural model.

Based on the above studies, since melt is the initial state when the intermetallic compounds form, the knowledge about the structure and the formation of the intermetallic phase in the melt can assist us in the synthesis and controlling of the intermetallic compounds in the materials. As one of the most typical intermetallic compounds, the $BiIn_2$ alloy is very attractive. It is known that its solidification behavior correlates with the structures of both the liquid and solid phases [20]. The viscosity coefficient shows the anomalous temperature dependence [21], which was supposed to be accompanied with concentration fluctuations in melt. In addition, the magnetic susceptibilities, electrical resistivities, and thermoelectric powers display anomaly near the concentration range of $BiIn_2$ [22]. It is widely accepted that the anomalous properties of the $BiIn_2$ are due to the self-associated atomic groups in the melt [21,23,24]. Moreover, the behaviors of these clusters can cause the structural changes of the melt [25]. However, the studies on the formation of the intermetallic clusters and their local structures are scarce, which are important for understanding the behaviors of the melt structure and the anomalous properties. In our work, by means of the high temperature X-ray diffraction [26], the liquid structure of the $BiIn_2$ intermetallic alloy has been detected. With the Extended X-ray Absorption Fine Structure (EXAFS) technique [27], the local structure around In atoms of the melt-quenched $BiIn_2$ intermetallic alloy ribbon has been obtained. The formation and evolution of the intermetallic clusters from the melt to the as-quenched crystalline state have been

* Corresponding author. Tel.: +86 531 88392748; fax: +86 531 88395011.
E-mail address: xfbian@sdu.edu.cn (X. Bian).
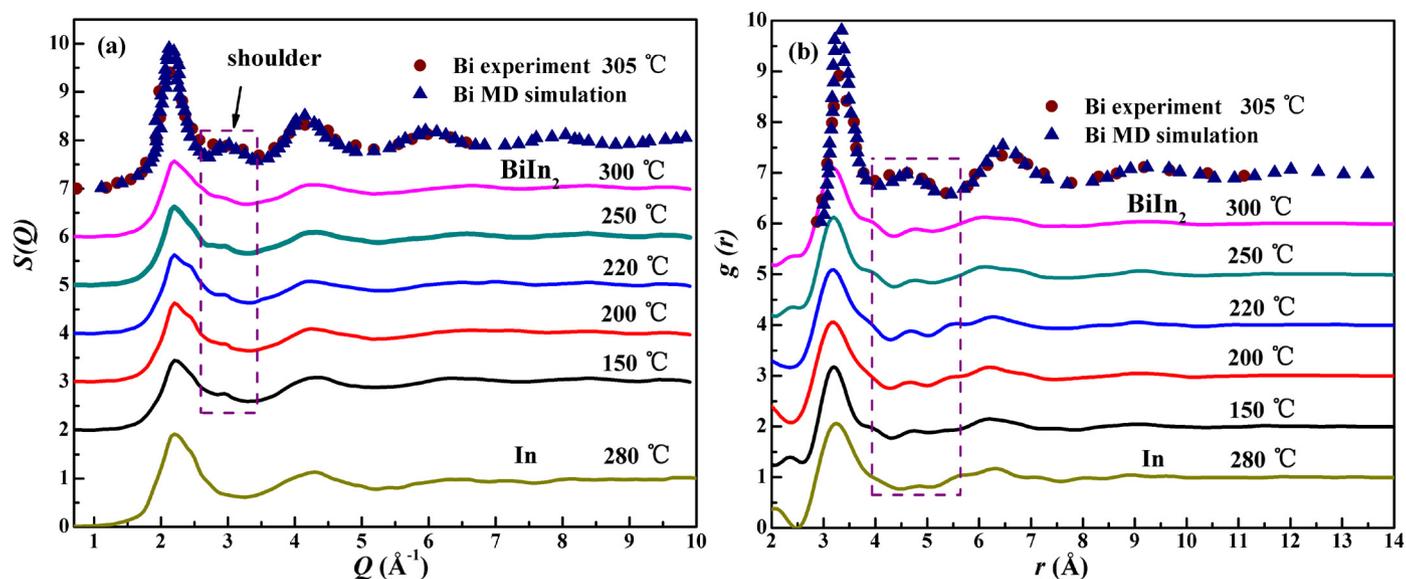
Fig. 1. (a) The structure factors $S(Q)$ of the pure Bi melt at 305 °C [30], pure In melt at 280 °C [31], and BiIn$_2$ alloy melt from 90 to 300 °C. (b) The pair distribution functions $g(r)$ of the pure Bi melt at 305 °C [30], pure In melt at 280 °C [31], and BiIn$_2$ alloy melt from 90 to 300 °C.

revealed. The structural differences between the melt and the as-quenched ribbon have been discussed, and the driven factors for the intermetallic alloy formation have been pointed out.

2. Experiments

The ingots of the BiIn$_2$ alloy were prepared by melting nominal amounts of pure Bi and In of 99.99% purity in a high frequency induction furnace under Ar atmosphere. X-ray diffraction measurements were carried out using a high temperature θ–θ type X-ray diffractometer. Mo Kα radiation (wavelength $\lambda = 0.7089$ Å) was reflected from the free surface of the specimen and reached the detector through a Zr monochromator in the diffraction beam. Experiments were performed at a high purity helium (99.999%) atmosphere of 2.0×10^{-5} Pa after the chamber was cleaned in vacuum of 1.0×10^{-3} Pa. The scanning voltage of the X-ray tube was 50 kV, the current was 40 mA, the exposure time was 5 s and the measured scattering angle 2θ was from 5° to 68°. The scanning step was 0.2°. The sample was held for 30 min to reach equilibrium every time before a new scattering scan started. The detailed data processing can be found in Ref. [28]. The error is less than 2% for r_1 by the adopted method.

The BiIn$_2$ intermetallic alloy ribbon was prepared by a single-roller melt-spinning technique with a circumferential speed of 27.5 m/s. The sample thickness is 40–50 μm. The In K-edge EXAFS spectra were measured at the beamline BL14W1 of Shanghai Synchrotron Radiation Faculty. The electron beam energy was 3.5 GeV and the maximum stored current was 300 mA. Data were collected by a fixed-exit double-crystal Si(311) channel-cut monochromator. The anterior ion chamber was filled with Ar, and the other with a mixture of Ar and Kr gases. The gases were used to detect incident X-ray intensity and transmitted intensity simultaneously. The energy resolution was 0.5×10^{-4}. The EXAFS data were analyzed using standard procedures with IFEFFIT code [29].

3. Results and discussion

3.1. The structure of the BiIn$_2$ intermetallic alloy melt

The structure factors $S(Q)$ of the pure In melt, pure Bi melt, and BiIn$_2$ intermetallic alloy melt at different temperatures are shown in Fig. 1(a). The first peaks in the $S(Q)$ curves of the BiIn$_2$

melt are asymmetrical. There is a shoulder on the high-Q side of the first peak of the BiIn$_2$ melt, which is similar to the $S(Q)$ curves of the pure Bi melt in Fig. 1(a) as well as in Refs. [32–34]. The shoulder on the $S(Q)$ curve is related to the interatomic potential [32] and the covalent bonds [35,36] in the melt. Comparatively, the intensity of the shoulder on the curve of the BiIn$_2$ melt is much weaker than that of the pure Bi melt. This suggests that the Bi–Bi covalent bonds in the pure Bi melt are largely reduced in the BiIn$_2$ melt. Fig. 1(b) shows the pair distribution functions $g(r)$ of the pure In melt, pure Bi melt, and BiIn$_2$ alloy melt at different temperatures. There are apparent humps between the first and the second peaks of the three melts, as marked in the dashed rectangle region. The shoulders on the high-r side of the first peaks can be observed clearly in the $g(r)$ curves of the BiIn$_2$ melt, while there is not any shoulder on the $g(r)$ curve of In. This indicates that the structure of the BiIn$_2$ melt is more complex, compared with that of the In melt. In addition, the profile of the $g(r)$ curve in the BiIn$_2$ melt changes with decreasing temperature, indicating the structure evolution of the intermetallic melt.

The structural parameters of the BiIn$_2$ alloy melt are shown in Fig. 2(a) and (b). From Fig. 2(a), the nearest neighbor distance r_1 (i.e., the position of the first peak in the $g(r)$) displays an increasing trend with decreasing temperature. This is due to the thermal contraction characteristic of In [31]. The values of r_1 are from 3.18 Å to 3.20 Å. Notice that, the atomic radii of In and Bi atoms are 1.67 Å and 1.63 Å, respectively. The r_1 are smaller than the sum of the atomic radii of In and Bi. Furthermore, r_1 of the alloy melt is smaller than that of pure In [31,33] and pure Bi [30,33] melts. The abnormally short bond length in the intermetallic alloy melt directly confirms the unexpected strong interactions between In and Bi atoms. Considering the nearest neighbor distances of Bi$_{23}$In$_{77}$ and Bi$_{13}$In$_{87}$ in Ref. [33] (which are all larger than that of the BiIn$_2$ melt), the increasing atomic fraction of Bi enhances the interactions between Bi–In bonds. However, the Bi$_{23}$In$_{77}$ and Bi$_{13}$In$_{87}$ alloys are not in the intermetallic compositions of the Bi–In system. This suggests that the Bi–In chemical bonds are tighter in the clusters with the intermetallic compound composition. Thus in the BiIn$_2$ melt, these chemical Bi–In bonds maintain the chemically ordered intermetallic clusters. The atom packing of the clusters with intermetallic compounds BiIn$_2$ in the melt deviates from the hard sphere random packing model [32,33].